

Short communication

Synthesis and electrochemistry of new layered $(1-x)$ $\text{LiVO}_2 \cdot x\text{Li}_2\text{TiO}_3$ ($0 \leq x \leq 0.6$) electrode materials

Lianqi Zhang^a, Kazunori Takada^{a,b,*}, Narumi Ohta^a,
Minoru Osada^a, Takayoshi Sasaki^{a,b}

^a *Nanoscale Materials Center, National Institute for Materials Science, Namiki 1-1, Tsukuba, Ibaraki 305-0044, Japan*

^b *Core Research for Evolutional Science and Technology (CREST), Japan Science and Technology Agency (JST),*

Honcho 4-1-8, Kawaguchi, Saitama 332-0012, Japan

Available online 26 June 2007

Abstract

Novel electrode materials with nominal compositions of $(1-x)\text{LiVO}_2 \cdot x\text{Li}_2\text{TiO}_3$ ($0 \leq x \leq 0.6$) were synthesized by carbothermal reduction reaction. All the materials were identified to have a layered structure and can be considered as a solid solution related to LiVO_2 – Li_2TiO_3 system, in which Li layers was alternately stacked with the layers made of mixture of Li, V, and Ti in a ccp array of oxygen. The redox reaction associated with vanadium ions was not reversible in LiVO_2 ; however, introduction of the redox couple into Li_2TiO_3 made it much more reversible. A reversible capacity of about 120 mAh g^{-1} remained after 90 cycles for the samples with $x=0.5$ and 0.6 , when they were cycled in the voltage range of 1.0–4.8 V.

© 2007 Elsevier B.V. All rights reserved.

Keywords: Lithium rechargeable battery; Layered structure; Solid solutions; $(1-x)\text{LiVO}_2 \cdot x\text{Li}_2\text{TiO}_3$

1. Introduction

The search for an alternative cathode material is still ongoing task. Recently, designing new electrode materials based on structural merger of layered LiAO_2 and Li_2MO_3 components to form a solid solution attracted much attention ($A=\text{Co}$ [1], Ni [2,7], Fe [3,8], Cr [4–6,9], and $\text{Ni}_{1/2}\text{Mn}_{1/2}$ [10,11]; $M=\text{Mn}$ and Ti). In these materials, Li_2MO_3 component was supposed to be electrochemically inert and act as a framework stabilizing the structure of LiAO_2 , resulting in the improvement of the cycling capability. The drastic improvements were reported for LiFeO_2 [3,8] and LiCrO_2 [4–6,9]. As well known, layered LiFeO_2 and LiCrO_2 showed extremely poor electrochemical reversibility [5–6,12]. However, incorporation of Cr^{3+} into inert Li_2MnO_3 [4–6] or Li_2TiO_3 [9] matrices, i.e. formation of LiCrO_2 – Li_2MO_3 ($M=\text{Mn}$, Ti) solid solution, stabilized the redox reaction against cycling, giving considerably high reversible capacity; similar effects were observed in LiFeO_2 – Li_2MnO_3 [3] and LiFeO_2 – Li_2TiO_3 [8] systems.

Among the well-known lithium 3D-transition metal oxides with layered structure, LiVO_2 as well as LiCrO_2 and LiFeO_2 quickly loses its electrode activity upon cycling, which was caused by the migration of vanadium ions from transitional metal layers to lithium layer during initial charge process [13]. The structural change prevents lithium ions from being back to their original sites, resulting in poor reversibility. Although such stabilization of LiVO_2 in layered Li_2MO_3 has not been reported so far to our best knowledge, the improvement of the electrode performance observed for LiCrO_2 and LiFeO_2 suggests that the redox reaction based on vanadium will be also reversible in layered solid solutions between layered LiVO_2 and Li_2MO_3 . $\text{V}^{3+}/\text{V}^{4+}$ redox couple is located at 3 V in LiVO_2 [13]. In the potential range, Li_2MnO_3 will not be an inert matrix because Mn^{4+} may be reduced to Mn^{3+} [11], and thus formation of LiVO_2 – Li_2MnO_3 solid solution is expected to be impossible. In contrast, Li_2TiO_3 with a low reduction potential of Ti^{4+} should behave as an electrochemically inactive matrix in the potential range. Therefore, Li_2TiO_3 was selected as the possible matrix by formation of LiVO_2 – Li_2TiO_3 solid solution. V^{3+} is usually formed in a reduction atmosphere [13], while Ti^{4+} can be maintained in an inert atmosphere and should be also able to co-exist with V^{3+} due to its low reduction potential [14], and thus carbothermal reduction method was adopted to form the solid solution in this work. In

* Corresponding author at: Nanoscale Materials Center, National Institute for Materials Science, Namiki 1-1, Tsukuba, Ibaraki 305-0044, Japan.
Tel.: +81 29 860 4317; fax: +81 29 854 9061.

E-mail address: takada.kazunori@nims.go.jp (K. Takada).

comparison with the conventional method of using H_2 or mixture of H_2 and Ar gases for preparing $LiVO_2$ [13,16], the carbothermal reduction method is more simple and cheaper [15]. The electrode properties were also investigated.

2. Experimental

$Li-V-Ti-O$ electrode materials were prepared by carbothermal reduction method [15]. A stoichiometric ratio of Li_2CO_3 , V_2O_5 , TiO_2 (rutile) and an appropriate amount of carbon in order to reduce V^{5+} in V_2O_5 to V^{3+} were mixed by ball-milling and heated at $1000^\circ C$ under an Ar gas flow for 20 h. After the heating, black product was found to be covered with a trace amount of yellow compound, which was identified as Li_3VO_4 by powder X-ray diffraction (XRD) and easily removed from the samples. For comparison, $LiVO_2$ and Li_2TiO_3 were also prepared by the same procedure. Samples were usually kept in an Ar-filled glove box.

The crystal structures of the samples were investigated by XRD. XRD data were collected on a diffractometer (RINT2200, Rigaku) with graphite-monochromatic $Cu K\alpha$ radiation ($\lambda = 0.15406$ nm). The contents of lithium, vanadium, and titanium in the samples were determined using an inductively coupled plasmas spectrometer (ICP-AES, SPS 1700HVR, Seiko Instruments, Japan), while carbon content was measured by a carbon-sulfur analyzer (LECO CS-444). Thermogravimetric-differential thermal analysis was carried out using Rigaku TGA-8120 instrument in the temperature range of $25-1000^\circ C$ at a heating rate of $5^\circ C min^{-1}$ in air.

The charge and discharge characteristics of $Li-V-Ti-O$ electrodes were examined in coin-type half-cells ($Li/Li-V-Ti-O$). The cathode consisted of 20 mg active material and 12 mg conductive binder [8 mg polytetrafluoroethylene (PTFE) and 4 mg acetylene black]. It was pressed on a titanium mesh at $300 kg cm^{-2}$ and then dried in an argon-filled glove box for 48 h. The electrolyte solution was a 1:1 mixture of ethylene carbonate (EC) and diethylcarbonate (DEC) containing 1 M $LiPF_6$. Cells were assembled in the glove box and cycled in the voltage ranges of 1.5–4.0 and 1.0–4.8 V at a constant current density of $0.23 mA cm^{-2}$ ($20 mA g^{-1}$).

3. Results and discussion

Fig. 1 shows XRD patterns of $(1-x)LiVO_2 \cdot xLi_2TiO_3$ ($0 \leq x \leq 1$). One of the end members, $LiVO_2$, has a layered $\alpha-NaFeO_2$ -type structure (Space group R-3m, No. 166) [16], in which Li and V layers are alternately stacked within a ccp array of oxygen. On the other hand, the other end member, Li_2TiO_3 , has a similar layered structure, in which Li and $(Li_{1/3}Ti_{2/3})$ layers are alternately stacked within a ccp array of oxygen [17]. All the strong reflections observed in the XRD were indexable based on the trigonal lattice as $LiVO_2$ and Li_2TiO_3 , and only regular shift of diffraction peaks with increasing x was observed. Lattice parameters, a and c , presented a linear change as shown in Fig. 2. These results lead to a conclusion that solid solutions with the similar layered structure to the two end members were formed, in which lithium layers are sandwiched by transition

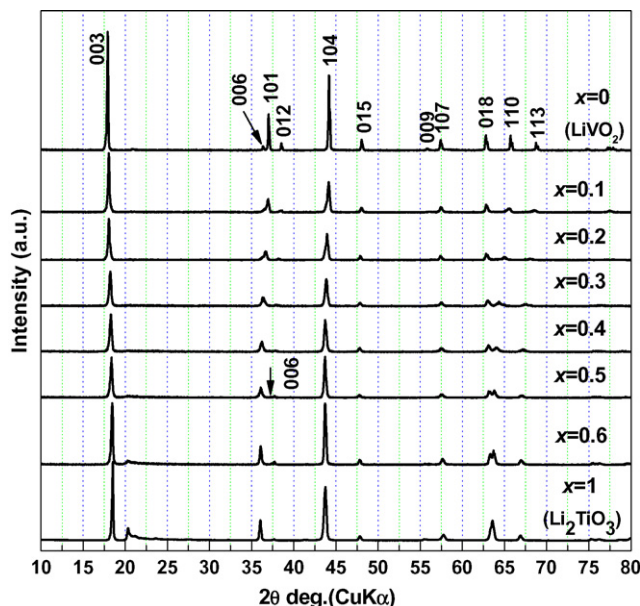


Fig. 1. XRD patterns of $(1-x)LiVO_2 \cdot xLi_2TiO_3$ ($0 \leq x \leq 0.6$) and Li_2TiO_3 . The reflections were indexed on the basis of space group R-3m.

metal layers comprising Li, V, and Ti. Increasing x developed a weak and broad band at around 20.3° and in the case of Li_2TiO_3 the reflections in the range became pronounced, which will be originated from cation ordering in the $(Li_{1/3}Ti_{2/3})$ layers.

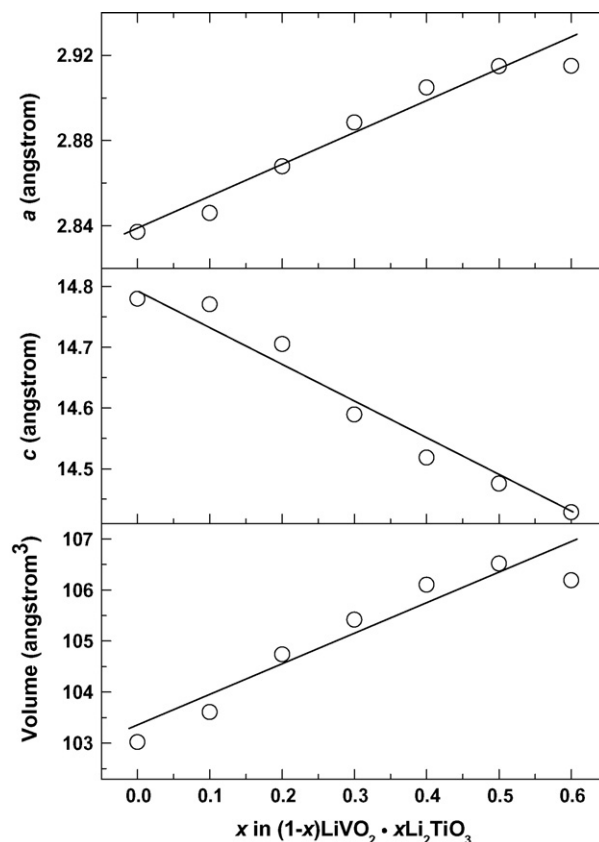


Fig. 2. Changes in lattice parameters and unit cell volume in a hexagonal unit cell for $(1-x)LiVO_2 \cdot xLi_2TiO_3$ ($0 \leq x \leq 0.6$).

Table 1
Results of chemical compositions analysis and initial coulombic efficiency in the voltage range of 4.0–1.5 V

| Samples | Analysis of chemical compositions | | | Initial coulombic efficiency (4.0–1.5 V) |
|----------------------------|---------------------------------------|---|---------------|--|
| | Molar ratio of Li/V/Ti (target value) | Molar ratio of [Li + V + Ti]/O (target value) | C content (%) | |
| $x=0$ (LiVO ₂) | 1.01/1 (1/1) | 0.88 (1.0) | 1.11 | 0.198 |
| $x=0.4$ | 3.36/1.49/1 (3.5/1.5/1) | 0.90 (1.0) | 0.7 | 0.483 |
| $x=0.5$ | 2.96/1.01/1 (3/1/1) | 0.92 (1.0) | 0.55 | 0.575 |
| $x=0.6$ | 2.59/0.65/1 (2.67/0.67/1) | 0.91 (1.0) | 0.51 | 0.599 |

The analyzed chemical compositions for several typical samples were listed in Table 1. Small amounts of carbon (less than 1% in weight, except for LiVO₂) still remained in the resulting materials. The Li/V/Ti ratios almost agreed with the expected values. However, when the oxygen contents were calculated by attributing the residual masses to oxygen, the samples always presented significant deviations in [Li + V + Ti]/O, which were lower than 1. The average valences of vanadium calculated on the basis of the compositions and tetravalent state of Ti were over +3. The thermal analysis performed in order to estimate the valence state of V also indicated that the average valence of vanadium in the case of $x=0.5$ was +3.28, when it was calculated according to the method mentioned in Fig. 3.

Additionally, TG–DTA curves were also indicative of possible chemical instability in air for these samples, because the weight gain during heating slowly proceeded even at a considerably lower temperature. In fact, the materials were gradually decomposed even in the storage at room temperature. This can be testified in Fig. 4. Fig. 4 shows XRD patterns of the samples after storage in air for about two months, clearly indicating that original structure of samples was not maintained with formation of additional phases. A basal reflection with a smaller d-spacing was observed for the sample with $x=0.1$. Weakened 003 reflections and lessened differences of the d-spacings between 018 and 110 reflections suggest increasing degree of cation disorder during the storage. Other additional reflections will be attributed

to Li₃VO₄, LiV₂O₅, Li₂CO₃, and LiOH. Therefore, the samples were usually kept in argon-filled glove box, and electrode drying was also carried out in argon-filled glove box. Prior to electrochemical examination, XRD patterns of several electrodes prepared in this work were taken in order to check if the structure of samples as electrode was maintained. Short-time exposure of samples to air did not destroy original layered structure.

Several typical samples were selected for electrochemical examination. Fig. 5 shows charge–discharge curves of $(1-x)\text{LiVO}_2 \cdot x\text{Li}_2\text{TiO}_3$ ($0.4 \leq x \leq 0.6$) cycled in the voltage ranges of 1.5–4.0 and 1.0–4.8 V and LiVO₂ as a comparison in the voltage range of 1.5–4.0 V. LiVO₂ indicated a charge plateau with around 90 mAh g⁻¹ in capacity at about 3 V, but lost most of the capacity in the following cycles. The potential was almost constant during the first charge, suggesting that the lithium deintercalation was accompanied by a phase transformation. It should be caused by migration of the vanadium ions to the Li layers, which makes the material electrochemically inactive [13]. The mergence of the LiVO₂ into Li₂TiO₃ made the first charge curve slanted, which strongly suggests that the phase transformation was suppressed in the LiVO₂–Li₂TiO₃ system. In fact, much more Li⁺ can be extracted especially for the sample with $x=0.4$. Increasing content of Li₂TiO₃ component also made an improved initial coulombic reversibility, as shown in Table 1, indicating that the V³⁺/V⁴⁺ redox couple becomes much more reversible than that in LiVO₂. The samples with $x=0.4$ and 0.5 delivered discharge capacities of about 100 mAh g⁻¹ when charged to 4.0 V.

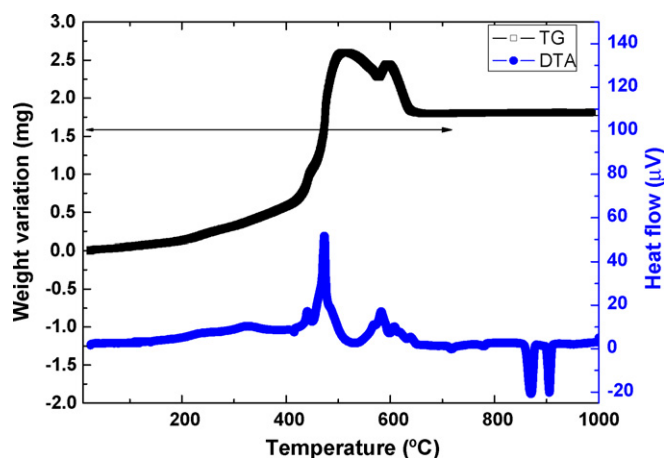


Fig. 3. TG–DTA curve of the sample with $x=0.5$. The average valence of vanadium was calculated to be +3.28 according to weight change in the range marked by the arrow in figure and the measured weight of metal ions by chemical composition analysis in the sample, assuming that V is finally oxidized to +5 and the remained carbon is removed.

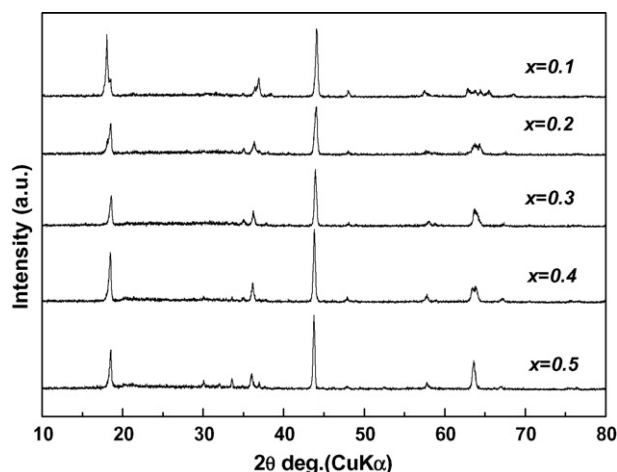


Fig. 4. XRD patterns of several samples after storage in air for about 60 days.

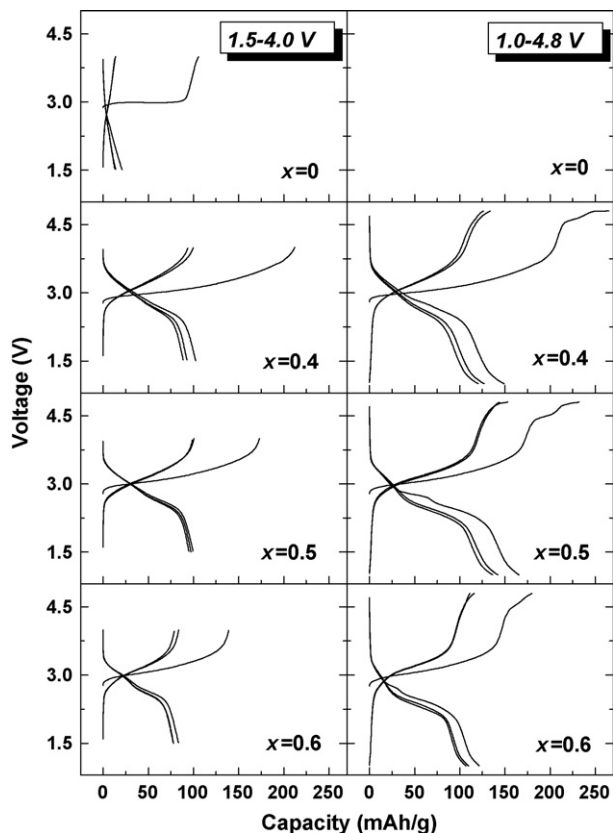


Fig. 5. Charge–discharge curves of $(1-x)\text{LiVO}_2 \cdot x\text{Li}_2\text{TiO}_3$ ($0.4 \leq x \leq 0.6$) cycled in the voltage range of 1.5–4.0 and 1.0–4.8 V at a constant current density of 0.23 mA cm^{-2} (20 mA g^{-1}) as well as LiVO_2 in the voltage range of 1.5–4.0 V.

Another interesting feature observed in $\text{LiCrO}_2\text{--Li}_2\text{MnO}_3$ system was an abnormally large capacity accompanying a long irreversible initial charge plateau at about 4.5 V, when it was charged up to 4.8 V [5–6]; but such a phenomenon was not observed for $\text{LiCrO}_2\text{--Li}_2\text{TiO}_3$ system. The present system only showed a small charge plateau at $>4.4 \text{ V}$ as shown in Fig. 5,

which slightly enlarged the initial reversible capacity to about 166 mAh g^{-1} in case of the sample with $x = 0.5$. The small charge plateau may mainly come from electrolyte decomposition. Ex situ or in situ XRD experiments to monitor change in lattice parameters during cycling may be helpful to confirm the origin of the potential plateau at the high voltage.

The cycleability for these materials is shown in Fig. 6. In the voltage of 1.5–4.0 V, all the samples gave similar cycleability. Even when they were cycled in the wider voltage range of 1.0–4.8 V, the samples still produced good cycling performance. Furthermore, increasing content of Li_2TiO_3 clearly improved long-term cycleability in the voltage range of 1.0–4.8 V. The sample with $x = 0.6$ did not show capacity fading and retained a capacity of 125 mAh g^{-1} after 90 cycles.

4. Conclusions

New layered electrode materials with the nominal compositions of $(1-x)\text{LiVO}_2 \cdot x\text{Li}_2\text{TiO}_3$ ($0 \leq x \leq 0.6$) were synthesized by carbothermal reduction reaction. XRD patterns indicated that they were isostructural to layered LiVO_2 or Li_2TiO_3 and considered as solid solution between them. The structural integration of LiVO_2 into an inert Li_2TiO_3 framework made the redox reaction associated with V ions much more reversible. A reversible capacity of about 120 mAh g^{-1} remained after 90 cycles for the samples with $x = 0.5$ and 0.6 , when they were cycled in the voltage range of 1.0–4.8 V. The improvement can be related to formation of a stable framework consisting of Ti^{4+} in materials, as deduced in some similar materials such as $\text{LiCrO}_2\text{--Li}_2\text{MO}_3$ systems.

Acknowledgements

The authors are grateful to Mr. S. Takenouchi of National Institute for Materials Science for the compositional analyses. This work was partially funded by Ministry of Economy, Trade and Industry (METI) and New Energy and Industrial Technology Development Organization (NEDO).

References

- [1] K. Numata, C. Sakaki, S. Yamanaka, Chem. Lett. 8 (1997) 725.
- [2] L. Zhang, H. Noguchi, M. Yoshio, J. Power Sources 110 (2002) 57.
- [3] M. Tabuchi, A. Nakashima, H. Shigemura, K. Ado, H. Kobayashi, H. Sakaebe, H. Kageyama, T. Nakamura, H. Kohzaki, A. Hirano, R. Kanno, J. Electrochem. Soc. 149 (2002) A509.
- [4] M. Balasubramanian, J. Mcbreen, I.J. Davidson, P.S. Whitfield, I. Kargina, J. Electrochem. Soc. 149 (2002) A176.
- [5] Z. Lu, J.R. Dahn, J. Electrochem. Soc. 149 (2002) A1454.
- [6] Z. Lu, J.R. Dahn, J. Electrochem. Soc. 150 (2003) A1044.
- [7] L. Zhang, X. Wang, H. Noguchi, M. Yoshio, K. Takada, T. Sasaki, Electrochim. Acta 49 (2004) 3305.
- [8] H. Shigemura, M. Tabuchi, H. Sakaebe, H. Kobayashi, H. Kageyama, J. Electrochem. Soc. 150 (2003) A638.
- [9] L. Zhang, H. Noguchi, J. Electrochem. Soc. 150 (2003) A607.
- [10] J.S. Kim, C.S. Johnson, M.M. Thackeray, Electrochem. Comm. 4 (2002) 205.
- [11] Z. Lu, L.Y. Beaulieu, R.A. Donabarger, C.L. Thomas, J.R. Dahn, J. Electrochem. Soc. 149 (2002) A778.

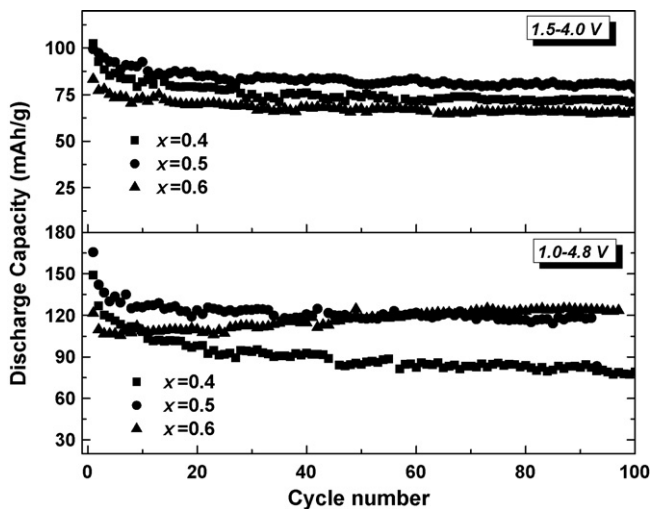


Fig. 6. Cycling performance of $(1-x)\text{LiVO}_2 \cdot x\text{Li}_2\text{TiO}_3$ ($0.4 \leq x \leq 0.6$) cycled in the voltage ranges of 1.5–4.0 and 1.0–4.8 V at a constant current density of 0.23 mA cm^{-2} (20 mA g^{-1}).

- [12] Y. Inada, R. Kanno, M. Takagi, Y. Takeda, *J. Electrochem. Soc.* 144 (1997) L177.
- [13] L.A. Piccioto, M.M. Thackeray, W.I.F. David, P.G. Bruce, J.B. Goodenough, *Mater. Res. Bull.* 19 (1984) 1497.
- [14] T. Ohzuku, A. Ueda, N. Yamamoto, *J. Electrochem. Soc.* 142 (1997) 1431.
- [15] J. Barker, M. Saidi, J.L. Swoyer, *J. Electrochem. Soc.* 150 (2003) A1267.
- [16] K. Kobayashi, K. Kosuge, S. Kachi, *Mater. Res. Bull.* 4 (1969) 95.
- [17] M. Castellanos, A.R. West, *J. Mater. Sci.* 14 (1979) 450.